Available online at www.sciencedirect.com
SCIENCE DIRECT®
ELSEVIER
International Journal of Multiphase Flow 30 (2004) 159–180
International Journal of Multiphase Flow
www.elsevier.com/locate/ijmulflow

An analytical approach for the closure equations of gas–solid flows with inter-particle collisions

Alexander Kartushinsky [a,1], Efstathios E. Michaelides [b,*]

[a] Estonian Energy Research Institute, 10137 Tallinn Paldiski Rd. 1, Estonia
[b] Department of Mechanical Engineering, School of Engineering, Tulane University, New Orleans, LA 70118-5674, USA

Received 16 April 2003; received in revised form 24 November 2003

Abstract

This work examines the effect of inter-particle collisions on the motion of solid particles in two-phase turbulent pipe and channel flows. Two mechanisms for the particle–particle collisions are considered, with and without friction sliding. Based on these collision mechanisms, the correlations of the various velocity components of colliding particles are obtained analytically by using an averaging procedure. This takes into account three collision coordinates, two angles and the distance between the centers of colliding particles. The various stress tensor components are obtained and then introduced in the mass, linear momentum and angular momentum equations of the dispersed phase. The current approach applies to particle–particle collisions that result from both the average velocity difference and the turbulent velocity fluctuations. In order to close the governing equations of the dispersed phase, the pseudo-viscosity coefficients are defined and determined by the time of duration of the inter-particle collision process. The model is general enough to apply to both polydisperse and monodisperse particulate systems and has been validated by comparisons with experimental data.

Keywords: Inter-particle collisions; Particulate flow; Pseudo-viscosity coefficients; Pipe flow

1. Introduction

A parameter that measures the importance of inter-particle collisions in a flowing gas–solid mixture is the ratio of the particle response time, β_{ui}^{-1}, to the time of inter-particle collisions, t_c. For

* Corresponding author. Tel.: +1-504-865-5764; fax: +1-504-862-8747.
E-mail addresses: kart@eeri.ee (A. Kartushinsky), emichael@tulane.edu (E.E. Michaelides).
[1] Tel.: +372-662-1822; fax: +372-661-3655.

0301-9322/$ - see front matter
doi:10.1016/j.ijmultiphaseflow.2003.10.007

dense particulate flows, $\beta_{ui}t_c < 1$, and particle-to-particle collisions must be taken into account. There are many theoretical studies on the subject of the inter-particle collision phenomena: Williams and Crane (1983) obtained an expression for the collision rate of the particles and their relative velocity in a turbulent flow in terms of the Stokes number. The Lagrangian approach of particle collisions was used by many researchers in the past including, more recently, Sommerfeld (2001) who introduced a stochastic inter-particle model when a fictitious particle and trace particles collide. Jenkins and Savage (1983) used a Eulerian approach that accounts for inter-particle collisions in the case of rapid granular flows. The so-called "granular temperature," which is an analog of the temperature obtained from a kinetic theory approach, may be calculated from the velocity distribution function of the particles. Other constitutive relations, also based on the kinetic theory, may be obtained by using the characteristic shape of the velocity distribution function. In the particular case of nearly elastic and frictionless inter-particle collisions this function may be assumed to be Maxwellian. In such a case, an expression for the total stress of the particles' collision may be obtained as in Louge et al. (1991) who used closure equations that involve the pseudo-viscosity coefficients and the stress tensor components corresponding to the collision terms in the transport equations of the dispersed phase.

In previous models for the closure of governing equations of the dispersed solid phase based on inter-particle collision (Hussainov et al., 1995; Frishman et al., 1997), an approximation was used (Babukha and Shraiber, 1972), that considers only one mechanism for the particle collisions, that is collision without sliding friction at the point of contact surfaces. These authors also took into account the effect of surface roughness by using an empirical roughness coefficient. This mechanism applies only to the motion of particles where the transverse component of the velocity is higher than the longitudinal (tangential) component at the moment of collision. It must be pointed out that the solution of such models cannot be achieved in the limiting case of the collision of identical particles because the computed pseudo-viscosity coefficients diverge since the time of inter-particle collisions becomes infinite.

Feng and Michaelides (2002) examined the drag on particles in the proximity of a wall. Matsumoto and Saito (1970) investigated particle–wall collisions and determined two mechanisms of interaction namely, collision with and without sliding friction at the point of surfaces contact. They also determined criteria for the application of these mechanisms. According to their investigation, if the ratio of transverse to tangential velocities is smaller than $2/[7f(1+k_n)]$ a collision with sliding friction is observed. Otherwise, a collision without sliding friction occurs and the tangential velocity is zero at the point of impact. The analyses of particle–wall and particle–particle collisions considering various stages of the collision process are presented in Crowe et al. (1998). They also considered separate expressions for the linear and angular velocity changes for both of these mechanisms.

In order to cover all plausible situations that may occur in a gas–solids flow, we developed a model that accounts for the mechanism of collision with sliding friction. Besides the improvement of the former models for inter-particle collision, an important motivation for the development of such a model is that it may be applied to identical particles without the divergence of the pseudo-viscosity or any other any parameter. With a sliding type of collision friction, we are able to reduce the terms related to the angular velocity in the expressions of the stress tensors in the linear–linear and linear–angular velocity correlations. This makes it possible to perform collision calculations for various sizes of particles that flow simultaneously in the mixture. Thus, the

present model is flexible to the variation of all the flow parameters and may also be applied in the case of polydisperse mixtures.

2. Closure of equations for dispersed particulate flows

The closure equations for the dispersed phase flow presented here are based on the inter-particle collision and are obtained by using a two-fluid model approach and an eddy-viscosity concept. The model describes the two-dimensional motion of the dispersed phase, when the particle angular velocity vector is normal to the plane of the translational motion of the particles. We have adopted this assumption for two reasons: (a) the equations of the model are simpler and less cumbersome to use, and (b) a great deal of the angular momentum of the particles is imparted by collisions with the walls of the flat channel. These collisions tend to align the angular velocity vector in a direction that is perpendicular to the plane of motion.

Following Crowe et al. (1998) the impulsive force exerted from particle "i" to particle "j" during the collision of two hard spheres may be decomposed into a normal unit vector, $\vec{e}$, directed towards the center of the first particle "i" and a tangential unit vector, $\vec{\tau} = \vec{G}_{ij}/|\vec{G}^{\mathrm{ct}}_{ij}|$. Hence, we have $\vec{J} = J_n\vec{e} + J_\tau\vec{\tau}$.

The following relation gives the condition for the importance of sliding friction collision:

$$\vec{e}\cdot\vec{G}_{ji}/|\vec{G}^{\mathrm{ct}}_{\mathrm{ji}}| < 2/7f(1+k_{pn}). \tag{1}$$

The tangential component of the impulsive force J_τ may be expressed in terms of the normal component J_n as $J_\tau = fJ_n$ with f being the Coulomb friction coefficient. The corresponding formulae for the translational and angular velocity changes of the two colliding particles "i" and "j" are given by Crowe et al. (1998) as follows:

$$\vec{v}'_i - \vec{v}_i = \beta_{ji}(1+k_{pn})(\vec{e} - f\vec{\tau})(\vec{e}\cdot\vec{G}_{ij}), \quad \vec{v}'_j - \vec{v}_j = -\beta_{ij}(1+k_{pn})(\vec{e} - f\vec{\tau})(\vec{e}\cdot\vec{G}_{ij}), \tag{2a}$$

and

$$\vec{\omega}'_i - \vec{\omega}_i = 5\beta_{ji}(1+k_n)(\vec{e}\cdot\vec{G}_{ij})(\vec{e}\times\vec{\tau})/\delta_i, \quad \vec{\omega}'_j - \vec{\omega}_j = 5\beta_{ij}(1+k_n)(\vec{e}\cdot\vec{G}_{ij})(\vec{e}\times\vec{\tau})/\delta_j. \tag{2b}$$

If condition (1) is not satisfied, then we have the following expressions:

$$\begin{aligned} &\vec{v}'_i - \vec{v}_i = \beta_{ji}\lfloor(1+k_{pn})(\vec{e}\cdot\vec{G}_{ij})\vec{e} + (2|\vec{G}^{\mathrm{ct}}_{\mathrm{ij}}|\vec{\tau}/7)\rfloor, \quad \vec{v}'_j - \vec{v}_j = -\beta_{ij}\lfloor(1+k_{pn})(\vec{e}\cdot\vec{G}_{ij})\vec{e} + (2|\vec{G}^{\mathrm{ct}}_{\mathrm{ij}}|\vec{\tau}/7)\rfloor, \\ &\vec{\omega}'_i - \vec{\omega}_i = -5\beta_{ji}|\vec{G}^{\mathrm{ct}}_{\mathrm{ij}}|(\vec{e}\times\vec{\tau})/3.5\delta_i, \quad \vec{\omega}'_j - \vec{\omega}_j = -5\beta_{ij}|\vec{G}^{\mathrm{ct}}_{\mathrm{ij}}|(\vec{e}\times\vec{\tau})/3.5\delta_j. \end{aligned} \tag{3}$$

The prime in the above expressions denotes the post-collision state.

The vectors $\vec{G}_{ij} = \vec{v}_j - \vec{v}_i$, $\vec{G}^{\mathrm{ct}}_{ij} = \vec{G}_{ij} - (\vec{G}_{ij}\cdot\vec{e})\vec{e} - 0.5(\delta_i\vec{\omega}_i + \delta_j\vec{\omega}_j)\times\vec{e}$ represent the relative particle velocity and its tangential component before the collision process respectively. The parameter $\beta_{ji} = m_j/(m_i+m_j)$ is the ratio of the colliding particle masses and k_{pn} is the restitution coefficient of the normal velocity components of the colliding particles. The direction of the unit vector $\vec{e}$ and the velocity changes of the particle "i" are characterized by three collision

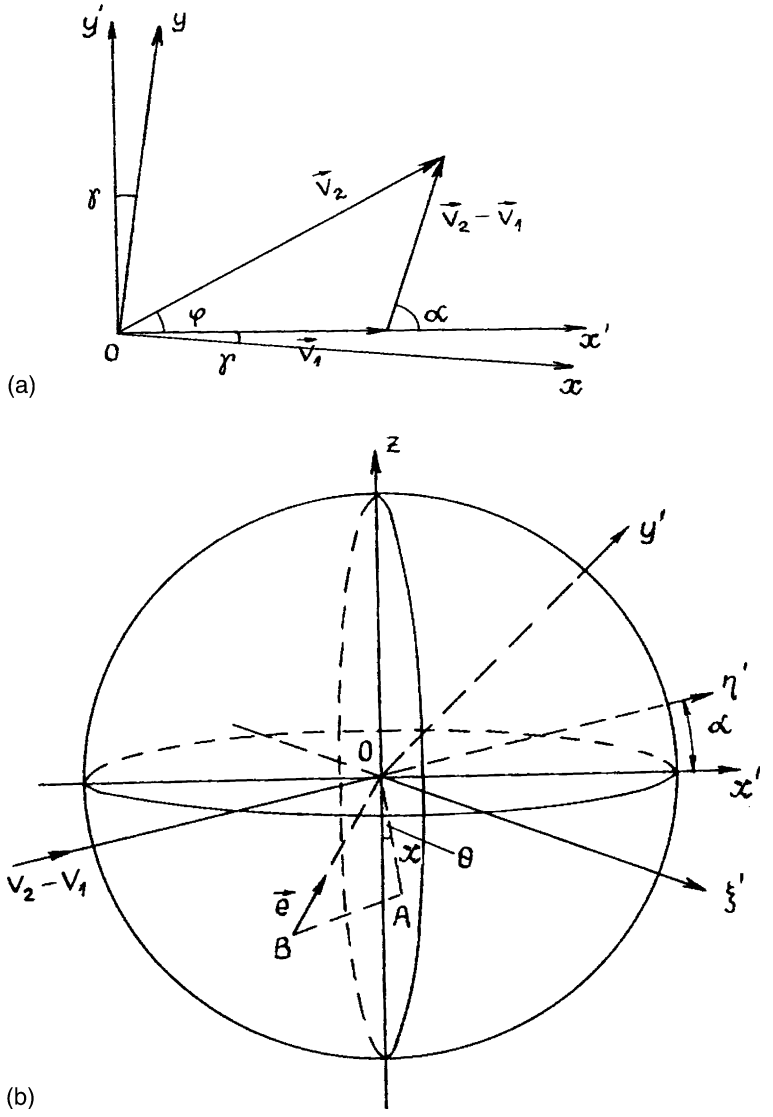

Fig. 1. Coordinates of the collision of two particles (a) on a plane and (b) in space.

coordinates, the distance x and the two angles θ, φ, which are depicted in Fig. 1a and b. Therefore, the expressions for the velocity differences of the two colliding particles may be written in the Cartesian coordinates as follows:

$$(\vec{V}'_i - \vec{V})_x \equiv u'_{si} - u_{si} = \beta_{ji}\cos\gamma_i \Big\{ (a - cx^2)(V_x - V_y tg\gamma_i) - cx\sqrt{1-x^2}\sin\theta(V_x tg\gamma_i + V_y) - \frac{b\omega_{ij}}{2\Delta_{ij}}[\sqrt{1-x^2}(V_x tg\gamma_i + V_y) + x\sin\theta(V_x - V_y tg\gamma_i)] \Big\}, \tag{4a}$$

$$(\vec{V}'_i - \vec{V})_y \equiv v'_{si} - v_{si} = \beta_{ji}\cos\gamma_i\Big\{(a - cx^2)(V_x tg\gamma_i + V_y) + cx\sqrt{1-x^2}\sin\theta(V_x - V_y tg\gamma_i) + \frac{b\omega_{ij}}{2\Delta_{ij}}[\sqrt{1-x^2}(V_x - V_y tg\gamma_i) - x\sin\theta(V_x tg\gamma_i + V_y)]\Big\}, \tag{4b}$$

$$(\vec{\omega}'_i - \vec{\omega}_i)_z \equiv \omega'_{si} - \omega_{si} = 5\beta_{ji} b\lfloor x\Delta_{ij}\sin\theta - 0.5\omega_{ij}(1 - (x\cos\theta)^2)\rfloor/\delta_i. \tag{4c}$$

Fig. 1a and b depict the plane and space diagrams of collision as they are used for the derivation of the equations. In the above expressions O, is the center of the particle "i" and B is the center of the particle "j," x is the projection of the inter-particle distance, $(\delta_i + \delta_j)/2$ onto the z-axis. The direction of the velocity difference $\vec{V}_2 - \vec{V}_1 \equiv \vec{V}_j - \vec{V}_i$ is along the coordinate line $O\eta'$ as shown in Fig. 1a and b. The other parameters are: $a = 1 + k_{pn}$, $b = 2/7$ (a parameter that accounts for the inertia of the spherical particle), and $c = a - b$. The angles γ_i and γ_j for both particles are determined from the ratio of the transverse velocity component to that of the longitudinal component $\tan\gamma_i = v_{si}/u_{si}$ and $\tan\gamma_j = v_{sj}/u_{sj}$.

It must be mentioned that the angle φ characterizes the difference in the motion of particles with different characteristics (particle fractions). In the case of the so called "fluctuating collisions," this angle varies in the range $0 \leqslant \varphi \leqslant 2\pi$ regardless to the motion of the particles. In the case of the "averaged collisions," this angle varies in the range $0 \leqslant \varphi \leqslant \varphi_{ij}$. In the latter case, the upper limit φ_{ij} is determined by the expression:$\tan\varphi_{ij} = \tan(\gamma_j - \gamma_i)$. Hence, the angle totally depends on the difference of the velocities of particle fractions that compose the solid phase. In the particular case of identical particles, $\varphi \equiv 0$.

The other collision coordinates vary in the ranges $0 \leqslant \theta \leqslant 2\pi$ and $0 \leqslant x \leqslant 1$. The calculations for the tangential velocity component in terms of the collision coordinates result in the expression $|\vec{G}^{ct}_{ij}| = \sqrt{(x\Delta_{ij})^2 - x\Delta_{ij}\sin\theta\omega_{ij} + 0.25(1 - x^2\cos^2\theta)\omega^2_{ij}} \equiv N$ and the scalar product of the normal vector to the vector of particles relative velocity becomes: $\vec{e}\cdot\vec{G}_{ij} \equiv \sqrt{1-x^2}\Delta_{ij}$.

The condition specified in Eq. (1) for the importance of collisions may be written as follows for the polydisperse mixture:

$$\left\langle \frac{\vec{e}\cdot\vec{G}_{ij}}{|\vec{G}^{ct}_{ij}|} \right\rangle_{\varphi,x,\theta} = \frac{\int_0^{\varphi_{ij}} d\varphi \int_0^1 x\sqrt{1-x^2}\,dx \int_0^{2\pi} \frac{\Delta_{ij} d\theta}{\sqrt{(x\Delta_{ij})^2 - x\Delta_{ij}\omega_{ij}\sin\theta + 0.25\omega^2_{ij}(1-(x\cos\theta)^2)}}}{2\pi\varphi_{ij}\int_0^1 x\,dx} < \frac{2}{7f(1+k_{pn})} \tag{5}$$

To simplify the description and to obtain analytically final expressions of tensor stresses for various velocity components we will evaluate the left-hand side of the inequality for three different cases of particle velocities, namely:

(a) The magnitude of the translational velocity of the colliding particles is much smaller than the angular velocity: $\Delta_{ij} \ll \omega_{ij}$.
(b) The translational velocity of colliding particles is of the same order of magnitude as the angular velocity: $\Delta_{ij} \approx \omega_{ij}$.
(c) The translational velocity of the colliding particles is much larger than the angular velocity: $\Delta_{ij} \gg \omega_{ij}$.

In the first case, the left-hand side of the inequality (7) is reduced to an integral that is equal to zero. In the second and third cases the inequality yields: $2\int_0^1 \sqrt{1-x^2}\,\mathrm{d}x = \frac{\pi}{2} < \frac{2}{7fa}$.

Therefore, when the magnitude of the translational velocity is much smaller than the angular velocity (case 1), sliding friction is important when

$$f \leqslant 4/(7\pi(1+k_{pn})). \tag{6}$$

Hence, the differences between the post- and pre-collision translation and angular velocities of the colliding particles may be obtained in terms of the collision coordinates as follows:

$$(\vec{v}_i' - \vec{v}_i)_x \equiv u_{si}' - u_{si} = \beta_{ji} a(A(V_x\cos\gamma_i - V_y\sin\gamma_i) - B(V_x\sin\gamma_i + V_y\cos\gamma_i)), \tag{7a}$$

$$(\vec{v}_i' - \vec{v}_i)_y \equiv v_{si}' - v_{si} = \beta_{ji} a(A(V_x\sin\gamma_i + V_y\cos\gamma_i) + B(V_x\cos\gamma_i - V_y\sin\gamma_i)), \tag{7b}$$

$$(\vec{\omega}_i' - \vec{\omega}_i)_z \equiv \omega_{si}' - \omega_{si} = 5\beta_{ji} fa\sqrt{1-x^2}\Delta_{ij}(e_z\tau_y - e_y\tau_z)/\delta_i = 5\beta_{ji} fa\sqrt{1-x^2}\Delta_{ij} C/\delta_i, \tag{7c}$$

The parameters A, B, C are calculated for the three cases described above as follows:

1. For the case $\Delta_{ij} \ll \omega_{ij}$,

$$A = 1 - x^2 + \frac{fx\sqrt{1-x^2}\sin\theta}{\sqrt{1-(x\cos\theta)^2}}, \quad B = x\sqrt{1-x^2}\sin\theta - \frac{f(1-x^2)}{\sqrt{1-(x\cos\theta)^2}}, \quad \text{and}$$

$$C = f\sqrt{1-(x\cos\theta)^2}\sqrt{1-x^2}\Delta_{ij}.$$

2. For the case $\Delta_{ij} \approx \omega_{ij}$,

$$A = 1 - x^2 - \frac{fx\sqrt{1-x^2}(x-\sin\theta)}{1-x\sin\theta}, \quad B = x\sqrt{1-x^2}\sin\theta - f(1-x^2), \quad \text{and}$$

$$C = f\left(1 - \frac{(x\cos\theta)^2}{1-x\sin\theta}\right)\sqrt{1-x^2}\Delta_{ij}.$$

3. For the case $\Delta_{ij} \gg \omega_{ij}$,

$$A = 1 - x^2 - fx\sqrt{1-x^2}, \quad B = \lfloor x\sqrt{1-x^2} + f(1-x^2)\rfloor\sin\theta, \quad \text{and}$$

$$C = -f\sqrt{1-x^2}\Delta_{ij}\sin\theta.$$

Hence, the velocity correlations are calculated as the product of the velocity differences of the various components by taking into account the subsequent averaged procedure over the three collision coordinates (φ, x, θ). Then one can determine the following six velocity correlations, by considering the sliding friction collision process in the case of any particle fraction, i, of a polydisperse mixture:

$$\begin{aligned}\langle(v_{si}' - v_{si})(u_{si}' - u_{si})\rangle|_{\varphi,x,\theta} = \beta_{ji}^2 a^2 (V_i + V_j)^2 \{&(0.5(\langle A^2\rangle - \langle B^2\rangle)\sin 2\gamma_i + \langle AB\rangle\cos 2\gamma_i)A_{ij} \\ &- 0.5\lfloor((\langle A^2\rangle - \langle B^2\rangle)\sin 2\gamma_i + 2\langle AB\rangle\cos 2\gamma_i)C_{ij} - ((\langle A^2\rangle \\ &- \langle B^2\rangle)\cos 2\gamma_i - 2\langle AB\rangle\sin 2\gamma_i)B_{ij}\rfloor\},\end{aligned} \tag{8a}$$

$$\langle (v'_{si}-v_{si})^2\rangle|_{\varphi,x,\theta} = \beta_{ji}^2 a^2 (V_i+V_j)^2 \{(\langle A^2\rangle \sin^2\gamma_i + \langle B^2\rangle \cos^2\gamma_i + \langle AB\rangle \sin 2\gamma_i)A_{ij} + 0.5\lfloor((\langle A^2\rangle - \langle B^2\rangle)\cos 2\gamma_i - 2\langle AB\rangle \sin 2\gamma_i)C_{ij} - ((\langle A^2\rangle - \langle B^2\rangle)\sin 2\gamma_i + 2\langle AB\rangle \cos 2\gamma_i)B_{ij}\rfloor\}, \tag{8b}$$

$$\langle (u'_{si}-u_{si})^2 + (v'_{si}-v_{si})^2\rangle|_{\varphi,x,\theta} = \beta_{ji}^2 a^2 (V_i+V_j)^2 (\langle A^2\rangle + \langle B^2\rangle)A_{ij}, \tag{8c}$$

$$\langle (v'_{si}-v_{si})(\omega'_{si}-\omega_{si})\rangle|_{\varphi,x,\theta} = \beta_{ji}^2 a^2 \frac{5(V_i+V_j)^2\cos\gamma_i}{\delta_i} \times [(\langle AC\rangle tg\gamma_i + \langle BC\rangle)L_{ij} - (\langle AC\rangle - \langle BC\rangle tg\gamma_i)M_{ij}], \tag{8d}$$

$$\langle (u'_{si}-u_{si})(\omega'_{si}-\omega_{si})\rangle|_{\varphi,x,\theta} = \beta_{ji}^2 a^2 \frac{5(V_i+V_j)^2\cos\gamma_i}{\delta_i} \times [(\langle AC\rangle - \langle BC\rangle tg\gamma_i)L_{ij} + (\langle AC\rangle tg\gamma_i + \langle BC\rangle)M_{ij}], \tag{8e}$$

and

$$\langle (\omega'_{si}-\omega_{si})^2\rangle|_{\varphi,x,\theta} = \beta_{ji}^2 a^2 \frac{25(V_i+V_j)^2\langle C\rangle^2}{\delta_i^2} A_{ij}. \tag{8f}$$

Hence, the averaged parameters for the three cases (a)–(c), considered are given by the following expressions:

1. For the first case,

$$\langle A^2\rangle|_{\varphi,x,\theta} = \frac{1}{3}+\frac{f^2}{10}, \quad \langle B^2\rangle|_{\varphi,x,\theta} = \frac{1}{12}+\frac{2f^2}{5}, \quad \langle AB\rangle|_{\varphi,x,\theta} = \langle AC\rangle|_{\varphi,x,\theta} \equiv 0,$$
$$\langle BC\rangle|_{\varphi,x,\theta} = -\frac{2f^2}{5}, \quad \text{and} \quad \langle C^2\rangle|_{\varphi,x,\theta} = \frac{5f^2}{12}.$$

2. For the second case,

$$\langle A^2\rangle|_{\varphi,x,\theta} = \frac{1}{3}-\frac{2f}{5}+\frac{f^2}{10}, \quad \langle B^2\rangle|_{\varphi,x,\theta} = \frac{1}{12}+\frac{f^2}{3}, \quad \langle AB\rangle|_{\varphi,x,\theta} = \frac{f}{15}(f-4),$$
$$\langle AC\rangle|_{\varphi,x,\theta} = \frac{f}{3}-\frac{f^2}{15}, \quad \langle BC\rangle|_{\varphi,x,\theta} = -f\left(\frac{1}{60}+\frac{f}{3}\right), \quad \text{and} \quad \langle C^2\rangle|_{\varphi,x,\theta} = \frac{9f^2}{20}.$$

3. For the third case,

$$\langle A^2\rangle|_{\varphi,x,\theta} = \frac{1}{3}-\frac{\pi f}{8}+\frac{f^2}{6}, \quad \langle B^2\rangle|_{\varphi,x,\theta} = \frac{1}{12}+\frac{\pi f}{16}+\frac{f^2}{6}, \quad \langle AB\rangle|_{\varphi,x,\theta} = \langle AC\rangle|_{\varphi,x,\theta} \equiv 0,$$
$$\langle BC\rangle|_{\varphi,x,\theta} = -\frac{f}{5}\left(\frac{2}{3}+f\right), \quad \text{and} \quad \langle C^2\rangle|_{\varphi,x,\theta} = \frac{f^2}{4}.$$

It must be pointed out that if the sliding friction is not of importance in the computations one has to apply the system of equations that do not take into account the sliding friction collision, that is to "switch off" the sliding friction from the system of closure equations. In the absence of sliding friction the velocity correlation equations may be obtained from Frishman et al. (1997).

The velocity correlations describe the influence of the collision forces on the motion of the particles. By the additional correlation of the square of the angular particle velocity one may determine the change of the angular velocity in the description of the inter-particle–particle collisions with respect to the "fluctuation part" of the collision procedure. We prefer to use the method of averaging because, by using the "average part" of the particles' collision process, it is rather easy to compute the parameters of the collision process from the average linear and angular velocities for the colliding particles. On the other hand, it is not as easy to do this in the absence of any knowledge of the fluctuations of the particle angular velocity. The expressions derived in this section facilitate the calculation of the parameters of the collision process as either the "average" or the "fluctuation components" in all cases.

3. Application of the closure equations to an eddy-viscosity model

We apply the closure equations for the collision process of particles to model for the transport equations of a polydisperse gas–solid mixture, which is based on a Boussinesq eddy-viscosity concept. By decomposing the general Boussinesq equation one may obtain the various terms for the closure transport equation of the polydisperse phase as described in the article by Frishman et al. (1997). Thus, one introduces into the model the pseudo-viscosity coefficients, $v_{si}^{x,y,\omega}$, in the linear and angular momentum equations of the dispersed phase. These coefficients are calculated by taking their respective averages over the collision coordinates, during the time of the collision, $t_{ij\mathrm{col}}$. In the case that the gas–solids mixture is composed of N solid's components $i = 1, 2, \ldots, N$, the pseudo-viscosity coefficients' expressions are calculated as follows:

$$v_{si}^{x} = \sum_{j=1, j\neq i}^{N} \langle (u'_{si} - u_{si})(v'_{si} - v_{si}) \rangle|_{\varphi,x,\theta} t_{ij\mathrm{col}}, \tag{9a}$$

$$v_{si}^{y} = \sum_{j=1, j\neq i}^{N} \langle (v'_{si} - v_{si})^2 \rangle|_{\varphi,x,\theta} t_{ij\mathrm{col}}, \tag{9b}$$

$$v_{si}^{\omega} = \sum_{j=1, j\neq i}^{N} \langle (\omega'_{si} - \omega_{si})(v'_{si} - v_{si}) \rangle|_{\varphi,x,\theta} \delta_i t_{ij\mathrm{col}}/2, \tag{9c}$$

and the collision diffusion coefficient:

$$D_{i\mathrm{col}} = 0.5 \sum_{j=1, j\neq i}^{N} \langle (\Delta u_{sij})^2 + (\Delta v_{sij})^2 \rangle|_{\varphi,x,\theta} t_{ij\mathrm{col}}. \tag{9d}$$

The time of the inter-particle collision may be given by the following expression (Marble, 1964):

$$t_{ij\mathrm{col}} = \frac{2\rho_p \delta_j^3}{3\rho\alpha_j(\delta_i + \delta_j)^2 |V_j - V_i|}, \tag{10}$$

where α_j is the mass concentration of the jth particle fraction and the velocity difference between the colliding particles in a polydisperse mixture is calculated from the integral:

$$|\vec{V}_j - \vec{V}_i| = \frac{\int_0^{\varphi_{ij}} \mathrm{d}\varphi \int_0^1 x\,\mathrm{d}x \int_0^{2\pi} \sqrt{V_i^2 + V_j^2 - 2V_iV_j\cos\varphi}\,\mathrm{d}\theta}{\pi\varphi_{ij}} \tag{11}$$

In the calculation of the time of inter-particle collisions we consider the decomposition process, which was outlined in the previous section, for the calculation of the magnitude of the velocity difference $|\vec{V}_j - \vec{V}_i|$. For the calculation of the velocity differences that stem from the fluctuating velocity components of the colliding particles we use the following conditions:

$$\varphi_{ij} \equiv 2\pi, \quad V_i = \sqrt{u_{si}'^2 + v_{si}'^2}, \quad \text{and} \quad V_j = \sqrt{u_{sj}'^2 + v_{sj}'^2}, \tag{12}$$

where u_{si}', v_{si}' are the fluctuating velocity components of the particle fraction, i. For the calculation of the velocity differences that stem from the average velocity components of the colliding particles we obtain the following conditions:

$$\tan\varphi_{ij} = \left|\left(\frac{v_{sj}}{u_{sj}} - \frac{v_{si}}{u_{si}}\right) \Big/ \left(1 + \frac{v_{si}v_{sj}}{u_{si}u_{sj}}\right)\right|, \quad V_i = \sqrt{u_{si}^2 + v_{si}^2}, \quad \text{and} \quad V_j = \sqrt{u_{sj}^2 + v_{sj}^2}, \tag{13}$$

where u_{si}, v_{si} denote the average velocity components of the colliding particle fractions.

4. Applications of the model

4.1. Governing equations

The approach described in Sections 2 and 3 is employed in order to model the behavior of a solid dispersed phase composed of three particle fractions with different sizes in an axisymmetric pipe flow with known mass fraction coefficients. It must be pointed out that, while we examine only three particle fractions, the model is general enough to be applied to any number of fractions. The governing equations for such a polydisperse mixture based on an Eulerian description may be written as follows:

$$\frac{\partial u}{\partial x} + \frac{1}{r}\frac{\partial (rv)}{\partial r} = 0, \tag{14a}$$

$$u\frac{\partial u}{\partial x} + v\frac{\partial u}{\partial r} = -\frac{\partial p}{\rho\partial x} + \frac{1}{r}\frac{\partial}{\partial r} r(\nu + \nu_t)\frac{\partial u}{\partial r} - \sum_{i=1}^{3} \alpha_i \frac{C_{Di}'}{\tau_i}(u - u_{si}), \tag{14b}$$

$$u\frac{\partial k}{\partial x} + v\frac{\partial k}{\partial r} = \frac{1}{r}\frac{\partial}{\partial r} r(\nu_t + \nu)\frac{\partial k}{\partial r} + \nu_t\left(\frac{\partial u}{\partial r}\right)^2 - \nu\left(\frac{\partial \sqrt{k}}{\partial r}\right)^2 + \sum_{i=1}^{3} \alpha_i \frac{C_{Di}'}{\tau_i}\left\{[(u - u_{si})^2 + (v - v_{si})^2] - \sum \langle u_{si}'u'\rangle|_{\mathrm{turb}}\right\} - \frac{k\sqrt{k}}{L_{\mathrm{h}}}, \tag{14c}$$

$$u_{si}\frac{\partial u_{si}}{\partial x}+\left(u_{si}-\frac{(D_{i\mathrm{col}}+D_{i\mathrm{turb}}+v_{si}^{x})}{\alpha_i}\frac{\partial\alpha_i}{\partial r}\right)\frac{\partial u_{si}}{\partial r}$$
$$=\frac{1}{r}\frac{\partial}{\partial r}r\left(v_{si}^{x}\frac{\partial u_{si}}{\partial r}\right)-\frac{\partial\alpha_i\langle u_{si}'^{2}\rangle_{\mathrm{col}}}{\alpha_i\partial x}-\frac{1}{r\alpha_i}\frac{\partial}{\partial r}r\alpha_i\langle u_{si}'v_{si}'\rangle_{\mathrm{turb}}+\frac{C_{Di}'}{\tau_i}(u-u_{si})$$
$$+C_{Mi}\Omega_i(v-v_{si})-g\left(1-\frac{\rho}{\rho_p}\right), \tag{14d}$$

$$u_{si}\frac{\partial v_{si}}{\partial x}+\left(v_{si}-\frac{(D_{i\mathrm{col}}+D_{i\mathrm{turb}}+v_{si}^{y})}{\alpha_i}\frac{\partial\alpha_i}{\partial r}\right)\frac{\partial v_{si}}{\partial r}$$
$$=\frac{1}{r}\frac{\partial}{\partial r}r\left(2v_{si}^{y}\frac{\partial v_{si}}{\partial r}-\frac{2k_{si}}{3}\right)-\frac{\partial\alpha_i\langle u_{si}'v_{si}'\rangle_{\mathrm{col}}}{\alpha_i\partial x}-\frac{1}{r}\frac{\partial\alpha_i\langle v_{si}'^{2}\rangle_{\mathrm{turb}}}{\alpha_i\partial r}+\frac{C_{Di}'}{b}\tau_i(v-v_{si})$$
$$-\left(C_{Mi}\Omega_i+F_{si}\,\mathrm{sgn}\left(\frac{\partial(u-u_{si})}{\partial r}\right)\right)(u-u_{si}), \tag{14e}$$

$$u_{si}\frac{\partial\omega_{si}}{\partial x}+\left(v_{si}-\frac{(D_{i\mathrm{col}}+D_{i\mathrm{turb}}+v_{si}^{\omega})}{\alpha_i}\frac{\partial\alpha_i}{\partial r}\right)\frac{\partial\omega_{si}}{\partial r}$$
$$=\frac{1}{r}\frac{\partial}{\partial r}r\left(v_{si}^{\omega}\frac{\partial\omega_{si}}{\partial r}\right)-\frac{\partial\alpha_i\langle\omega_{si}'u_{si}'\rangle_{\mathrm{col}}}{\alpha_i\partial x}-\frac{\partial\alpha_i\langle\omega_{si}'v_{si}'\rangle_{\mathrm{turb}}}{r\alpha_i\partial r}-\frac{C_{\omega i}}{\tau_i}\Omega_i, \tag{14f}$$

$$\frac{\partial(\alpha_i u_{si})}{\partial x}+\frac{1}{r}\frac{\partial(r\alpha_i u_{si})}{\partial r}=\frac{1}{r}\frac{\partial}{\partial r}r(D_{i\mathrm{col}}+D_{i\mathrm{turb}})\frac{\partial\alpha_i}{\partial r}, \tag{14g}$$

where u_{si}, v_{si}, ω_{si}, α_i are the longitudinal, transverse, angular averaged velocity and mass concentration of ith particle fraction respectively; u_{si}', v_{si}', u_{pi}', v_{pi}', are the fluctuation velocity components of particles, caused by both the inter-particle collisions and by turbulence; $v_{si}^{x,y,\omega}$ are the pseudo-viscosity coefficients; k_{si} is the energy exchanged during the particles' collisions; $D_{i\mathrm{turb}}$ is the turbulent diffusion coefficient; and $\Omega_i=\omega_{si}-0.5(\partial u/\partial r-\partial v/\partial x)$ is the angular velocity slip. The other coefficients of the governing equations are defined as follows:

$$\nu_t=C_{\mu t}\sqrt{k}L_{\mathrm{T}}, \tag{15a}$$

$$\varepsilon=k\sqrt{k}/L_{\mathrm{T}}, \tag{15b}$$

$$C_{\mu t}=0.07(L_{\mathrm{T}}\sqrt{k})\exp\lfloor-2.5/(1+(L_{\mathrm{T}}\sqrt{k}/50\nu))\rfloor, \tag{15c}$$

and

$$L_{\mathrm{h}}=2L_{\mathrm{T}}\lambda/(L_{\mathrm{T}}+\lambda). \tag{15d}$$

For the drag coefficient, we use the Shiller and Naumann (1933) expression for the drag multiplier $f=1+0.15Re_{si}^{0.687}$. The characteristic time of the particles is $\tau_i^{-1}=18\mu/\rho_p\delta_i^2$. The Reynolds number due to fluctuations is $Re_{si}=\delta_i\sqrt{(u-u_{si})^2+(v-v_{si})^2}/\nu$, where δ_i is the diameter of particles in the fraction i.

The coefficients for the calculation of the Magnus lift force and torque, C_{Mi} and $C_{\omega i}$, may be obtained from Rubinow and Keller (1961) for small Reynolds numbers, or from Yamomoto et al. (2001) for larger Reynolds numbers.

In the case of shear flow we also use the expressions for the lift derived by Saffman (1965) and extended by Mei (1992) to higher Reynolds numbers. Alternatively, one may use the more recent expression by Thorncroft et al. (2001) for the shear lift force (Michaelides, 2003).

The parameter β_i is given by the following expression:

$$\beta_i = \frac{1}{2}\left(\frac{\partial u}{\partial r} - \frac{\partial u_{si}}{\partial r}\right)\frac{\delta_i}{\sqrt{(u-u_{si})^2 + (v-v_{si})^2}}. \tag{16}$$

The value of this parameter varies in the range $0.005 < \beta < 0.4$. Of the other parameters in the governing equations, g is the gravitational force, L_h is the hybrid turbulence length scale, which is equal to the inter-particle distance, $\lambda = \delta_\Sigma \lfloor (\pi\rho_p/6\rho\alpha_\Sigma)^{1/3} - 1 \rfloor$ and L_T is the integral turbulence length scale of the single-phase flow: $L_T = \frac{k_0^{3/2}}{\varepsilon_0}$.

4.2. Other parameters used in the model

The governing system of equations for the dispersed phase is solved for each of the three particle fractions ($i = 1, 3$). The factors that are affected by the particles motion and, which are taken into account in the computations, are the following:

4.2.1. Turbulence parameters

A two-way coupling model is used that contains with only one differential equation for k presented by Crowe and Gillandt (1998). We purposely applied this model in so-called truncated form, rather than the older $k-\varepsilon$ turbulence model, because the model enables one to account for the turbulence modulation caused by the presence of particles. Turbulent energy is produced by the average velocity lag between the two phases and is proportional to square of the velocity lag. To balance the growth of such additional turbulence energy, one may introduce in a semi-empirical manner an increased value of the dissipation rate, which is determined by the hybrid length scale L_h (Crowe and Gillandt, 1998). The latter is the harmonic average of the integral turbulence scale of single-phase flow and inter-particle distance. Since the hybrid length scale has the limitation that for very dilute flows, $L_h \to 2L_T$, in the actual computations we switch to $L_h \equiv L_T$ whenever the mass loading is less than 0.01.

The turbulence attenuation may be described by the sum of the correlations of the various particle-gas velocity components (Yuan and Michaelides, 1992):

$$\sum_{\substack{k=x,y \\ l=y,x}} \langle u'_{sik} u'_l \rangle|_{\text{turb}} = \langle u'_{si} u' \rangle|_{\text{turb}} + \langle v'_{si} u' \rangle|_{\text{turb}} + \langle u'_{si} v' \rangle|_{\text{turb}} + \langle v'_{si} v' \rangle|_{\text{turb}}. \tag{17}$$

The direct influence of the turbulence on the motion of the particles is through the velocity fluctuations $\langle u'_{si} v'_{si} \rangle_{\text{turb}}$, $\langle v'^2_{si} \rangle_{\text{turb}}$, $\langle \omega'_{si} v'_{si} \rangle_{\text{turb}}$. Expressions for the fluid-particle and particle–particle turbulent fluctuating velocity correlations that are caused by the turbulent fluctuations of the fluid velocity are given by Shraiber et al. (1990).

4.2.2. Particle-to-particle interactions

The influence of particle interactions may be described by the pseudo-viscosity coefficients v_{si}^{x}, v_{si}^{y}, v_{si}^{ω} and $D_{i\mathrm{col}}$ for the linear momentum equations in the axial and radial directions, the angular momentum equation and the continuity equation of the dispersed phase as well as by the stress tensor components $\langle u_{si}'^2\rangle_{\mathrm{col}}$, $\langle u_{si}'v_{si}'\rangle_{\mathrm{col}}$, $\langle \omega_{si}'v_{si}'\rangle_{\mathrm{col}}$. Considering the particle collisions effect on the particle motion, two specific effects are taken into account:

- The collisions that result in the fluctuation of the particle velocity components, which are caused by the turbulent fluctuations of the carrier fluid and,
- The collisions that are taken into account in the average velocity differences. These are due to the differences in the average velocity of the particle fractions.

Therefore, all the pseudo-viscosity coefficients as well as the tensor components would consist of two parts, the average and the fluctuation parts, which may be written as follows:

$$\begin{aligned}
&v_{si}^{x} = v_{si}^{x\mathrm{fluc}} + v_{si}^{x\mathrm{aver}}, \quad v_{si}^{y} = v_{si}^{y\mathrm{fluc}} + v_{si}^{y\mathrm{aver}}, \quad v_{si}^{\omega} = v_{si}^{\omega\mathrm{fluc}} + v_{si}^{\omega\mathrm{aver}},\\
&D_{i\mathrm{col}} = D_{i\mathrm{col}}^{\mathrm{fluc}} + D_{i\mathrm{col}}^{\mathrm{aver}}, \quad k_{si} = k_{si}^{\mathrm{fluc}} + k_{si}^{\mathrm{aver}}, \quad \langle u_{si}'^2\rangle_{\mathrm{col}} = \langle u_{si}'^2\rangle_{\mathrm{col}}^{\mathrm{fluc}} + \langle u_{si}'^2\rangle_{\mathrm{col}}^{\mathrm{aver}},\\
&\langle u_{si}'v_{si}'\rangle_{\mathrm{col}} = \langle u_{si}'v_{si}'\rangle_{\mathrm{col}}^{\mathrm{fluc}} + \langle u_{si}'v_{si}'\rangle_{\mathrm{col}}^{\mathrm{aver}}, \quad \langle \omega_{si}'u_{si}'\rangle_{\mathrm{col}} = \langle \omega_{si}'u_{si}'\rangle_{\mathrm{col}}^{\mathrm{fluc}} + \langle \omega_{si}'u_{si}'\rangle_{\mathrm{col}}^{\mathrm{aver}}.
\end{aligned} \tag{18}$$

4.2.3. Forces acting on particles

The various forces acting on the mixture are the viscous drag force, the gravitational force and the lift forces, which were described in Section 4.1.

4.2.4. Effect of particles' concentration/rarefaction

Since the particle distribution across the pipe is non-uniform because of the radial forces, we use the concept of the particle mean free path, suggested by Louge et al. (1991), in order to correct for the inhomogeneities due to the particles. Thus, the pseudo-viscosity coefficients $v_{si}^{x,y,\omega}$, the diffusion coefficient $D_{i\mathrm{col}}$ and the stress tensor components due to the collision k_{si}, $\langle u_{si}'^2\rangle_{\mathrm{col}}$, $\langle u_{si}'v_{si}'\rangle_{\mathrm{col}}$, $\langle \omega_{si}'u_{si}'\rangle_{\mathrm{col}}$ are multiplied by the factor $f_\gamma = 1/(1+\gamma/R)$ where γ is the mean free path of the particles and R is the pipe radius.

4.2.5. Boundary conditions

We consider that particles enter the flow domain of a steady-state single-phase turbulent pipe flow. The initial velocity for the dispersed phase is given in terms of a lag, or slip coefficient k_{lag} as follows:

$$\text{at } x = 0: \quad u_{si} = k_{\mathrm{lag}}u, \quad v_{si} = k_{\mathrm{lag}}v, \quad \omega_{si} = k_{\mathrm{lag}}(0.5\,\mathrm{rot}\,\vec{v}), \tag{19a}$$

The lag coefficient k_{lag} is calculated from the terminal velocities of the different particle fractions. Thus the particle mass concentration is calculated from the mass loading, which initially is assumed to be uniform across the cross-section of the pipe.

$$\text{at } x = 0: \quad \alpha_i = \psi k_{\mathrm{fri}}\bar{u}/\bar{u}_{si}. \tag{19b}$$

In the last equation, ψ is the mass loading, $\bar{u}$ and $\bar{u}_{si}$ are the average velocities of the gas-phase and particles over the cross-section at $x = 0$, and $k_{\mathrm{fr}i}$ is the initial fractional coefficient of the "ith" particle fraction ($\sum_{i=1,3} k_{\mathrm{fr}i} = 1$).

In the case of the upward pipe flow that is considered here, the boundary conditions at the axis are the axisymmetric conditions:

$$r = 0: \quad \frac{\partial u}{\partial r} = \frac{\partial k}{\partial r} = \frac{\partial u_{si}}{\partial r} = \frac{\partial \alpha_i}{\partial r} = v = v_{si} = \omega_{si} = 0. \tag{19c}$$

At the wall, for the gaseous phase we have the no-slip conditions:

$$r = R: u = v = k = 0. \tag{19d}$$

For the dispersed phase the boundary conditions at the wall are determined by using the following conditions, derived by Matsumoto and Saito (1970):

A. If $v_{si} > 0$ that is the particles are about to collide with the wall:

For $\left|u_{si} - \frac{\delta_i \omega_{si}}{2}\right| > \frac{7}{2}\mu_0(1 + k_n)v_{si}$,

$$u''_{si} = u_{si} + \mu_d \operatorname{sgn}\left(u_{si} - \frac{\delta_i \omega_i}{2}\right) v_{si}, \tag{19e}$$

$$\omega''_{si} = \omega_{si} + 5\mu_d \operatorname{sgn}\left(u_{si} - \frac{\delta_i \omega_i}{2}\right) \frac{v_{si}}{\delta_i}, \tag{19f}$$

$$v''_{si} = k_n v_{si}. \tag{19g}$$

For $\left|u_{si} - \frac{\delta_i \omega_{si}}{2}\right| \leqslant \frac{7}{2}\mu_0(1 + k_n)v_{si}$,

$$u''_{si} = u_{si} - \frac{2}{7}\left(u_{si} - \frac{\delta_i \omega_i}{2}\right), \tag{19h}$$

$$\omega''_{si} = \omega_{si} - \frac{10}{7\delta_i}\left(u_{si} - \frac{\delta_i \omega_i}{2}\right), \tag{19i}$$

$$v''_{si} = k_n v_{si}. \tag{19j}$$

Finally, the linear and angular velocity components of the particle fractions are calculated by means of the post-collision and pre-collision velocity components:

$$u_{si} = 0.5(u'_{si} + u_{si}), \quad \omega_{si} = 0.5(\omega''_{si} + \omega_{si}), \quad v_{si} = 0.5(v''_{si} + v_{si}). \tag{19k}$$

B. If $v_{si} \leqslant 0$ and the particles do not collide with the wall, the simpler conditions are used:

$$u_{si} = -\gamma_i \frac{\partial u_{si}}{\partial r}, \quad \omega_{si} = \gamma_i \frac{\partial \omega_{si}}{\partial r}, \quad v_{si} = 0, \tag{19l}$$

where γ_i is the mean free path of the particles, which is given by the expression:

$$\gamma_i = \frac{\rho_p \delta_i}{6\rho\left(\alpha_i + \sum_{j=1,3,j\neq i} \frac{\alpha_j \delta_i}{4\delta_j}\left(1 + \frac{\delta_i}{\delta_j}\right)^2\right)}. \tag{19m}$$

This takes into account the changes of the free path of the ith particle fraction due to the collisions with the other two particle fractions. It must be pointed out that the last boundary condition

implies that there is a velocity slip along the wall as suggested by Crowe et al. (1996). In this case, it is reasonable to consider that the sign of the derivatives signifies that the longitudinal particle velocity decreases towards the wall and that the angular velocity of the particles increases towards the wall.

It must be pointed out that the correction for the mean free path takes into account the small changes of the particle velocity due to the gradients of the velocity field at the wall. For the numerical computations, this mean free particle path must be much larger than the mesh size of the numerical grid.

The boundary condition for the particle mass concentration at the wall is determined by the conservation equation for the particle masses:

$$r = R: \quad \alpha_i v_{si} = (D_{i\mathrm{col}} + D_{i\mathrm{turb}}) \frac{\partial \alpha_i}{\partial r}. \tag{19n}$$

In the numerical implementation of the model, the boundary conditions for the dispersed phase are not strictly applied at the wall, but very close to it, at a distance equal to one particle diameter. This is very important in the calculations of the transport of rough particles whose sizes exceed the width of the viscous sub-layer and partially overlap the buffer zone. If this is not taken into account, then particles may overlap with the wall. Because of this, the flow domain for the dispersed phase is slightly narrower than that of the gaseous phase (Hussainov et al., 1996).

5. Numerical results and discussion

For the numerical calculations, a non-uniform grid is used in a three-layer model composed of the turbulent core, the buffer zone and the laminar sub-layer. The same numerical grid is used for the dispersed phase, with the exception that near the wall the grid is shorter by one particle size. A standard tri-diagonal algorithm with a six-point formula and an up-wind difference scheme is used for the solution of the partial differential equations. The adjustable constants in the model are as follows: $k_{pn} = 0.68$, $k_n = 0.9$, $f = 0.237$, $\mu_0 = 0.2$ and $\mu_d = 0.2$ and they were applied under all the conditions of the computations presented here. Standard values for pipe flow are assumed for the coefficient of the turbulence model, $C_{\mu t}$, C_{t1}, C_{t2} and C_{t3}.

For the validation of the model, calculations were performed to compare the numerical results with the experimental data by Tsuji et al. (1984), which have become the standard of comparison for gas–solid flows. The experiments are for vertical polystyrene particles, with the following properties and flow parameters:

A. $D = 30.5$ mm, $L = 5100$ mm, $\bar{u} = 10.7$ m/s, $\psi = 1.9$ kg/kg, $\rho_p = 1020$ kg/m^3, $\delta = 243$ μm;
B. $D = 30.5$ mm, $L = 5100$ mm, $\bar{u} = 10.7$ m/s, $\psi = 3.4$ kg/kg, $\rho_p = 1020$ kg/m^3, $\delta = 501$ μm.

The results of the calculations are shown in Fig. 2. It is observed that there is excellent agreement between the experimental data and the numerical results of the particulate flow as well as the single-phase flow. The numerical data even reproduce the off-center velocity maximum point at $r/R = 0.5$ in the mixture carrying the bigger particles. This reproduction of such a salient feature is impossible without an accurate inter-particle collision model.

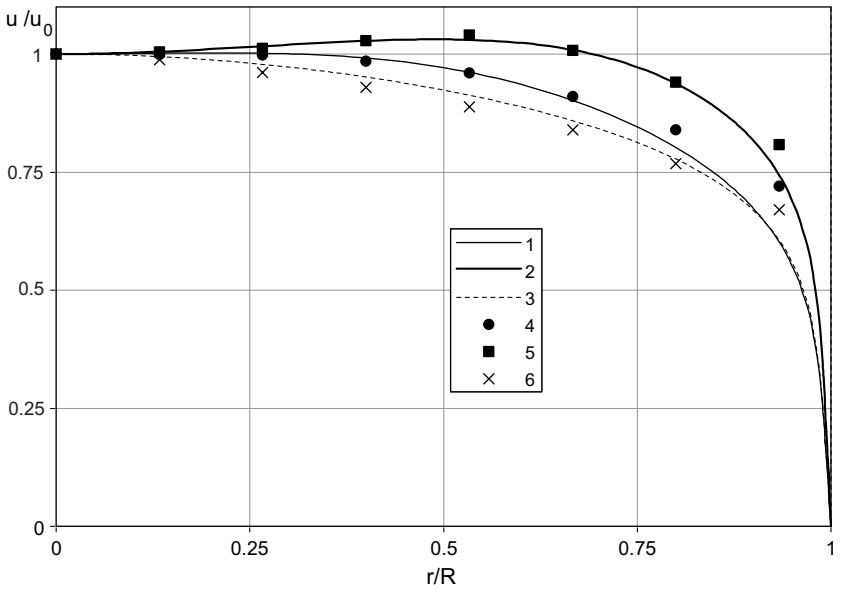

Fig. 2. Profiles of the longitudinal velocity component of the carrier fluid with particles: $\delta = 243$ μm (curve 1), $\delta = 501$ μm (curve 2), and carrier fluid alone (curve 3). The experimental data are from Tsuji et al. (1984).

Fig. 3 shows the distributions of the longitudinal velocity component of the gaseous phase as well as of the dispersed phase and the experimental data that correspond to the computed distributions. It is observed that the larger particles have higher average velocity slip a feature that is expected in vertical flows. It must be pointed out that the agreement between the computed and the experimental curves for the heavier particles does not appear to be as good as the others. This may be due to experimental error or to an underestimation of the terminal velocity of the particles, which was not reported and is necessary to be used in the model.

We also run numerical calculations without taking into consideration the particle–particle collisions and show the results in Fig. 4. It is observed that neglecting the collisions results in an uneven distribution of the particle velocity close to the wall. In the rest of the flow field the results are reasonable and appear to be close to the results obtained in the case of collisions. This leads us to conclude that, at least in vertical pipes, the model of the inter-particle collisions has a smoothing effect on the velocity computations near the boundaries of the flow. Given that inter-particle collisions also smoothen the concentration distribution of the particles, this is a reasonable and expected result. A glance at the last two figures shows that the particle velocity at the walls is underestimated. This may be due to two reasons: (a) either the boundary conditions used are not adequate and, therefore, more research is needed on a proper set of boundary conditions at the wall, or (b) to experimental error, which is higher than normal close to the wall.

Fig. 5 depicts the transverse velocity components for two particle fractions with particle sizes $\delta = 243$ and 501 μm. The velocities are normalized by the fluid friction velocity: $\bar{v}_s = v_s/u_*$.

It is apparent from the results depicted in Figs. 2–4 that the particle phase lags the gaseous phase and that there is a small-magnitude particle migration towards the center of the pipe. This is confirmed by the computation of the particle transverse velocity shown in Fig. 5 and from the

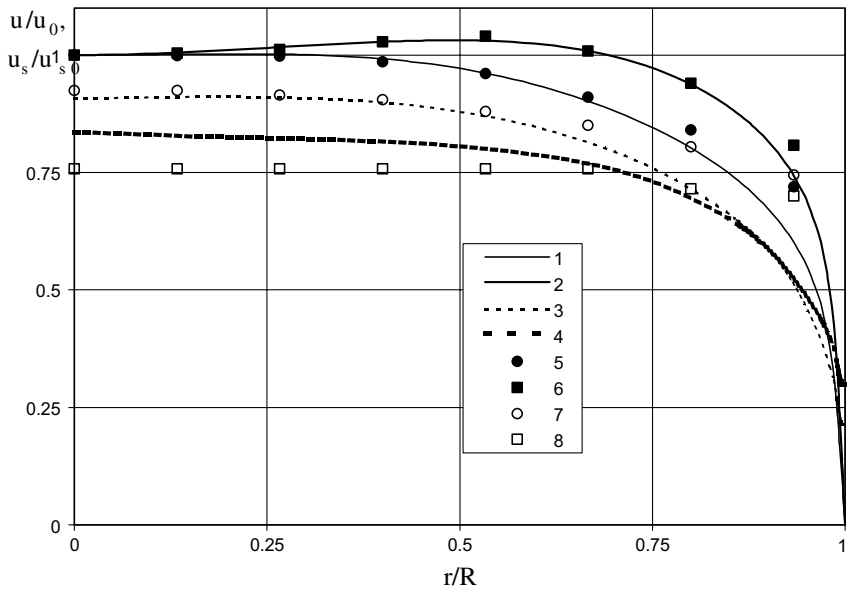

Fig. 3. Profiles of the longitudinal velocity component of the carrier fluid with particles: $\delta = 243$ μm (curve 1), $\delta = 501$ μm (curve 2); and longitudinal velocity of particles: $\delta = 243$ μm (curve 3), $\delta = 501$ μm (curve 4). The experimental data are from Tsuji et al. (1984).

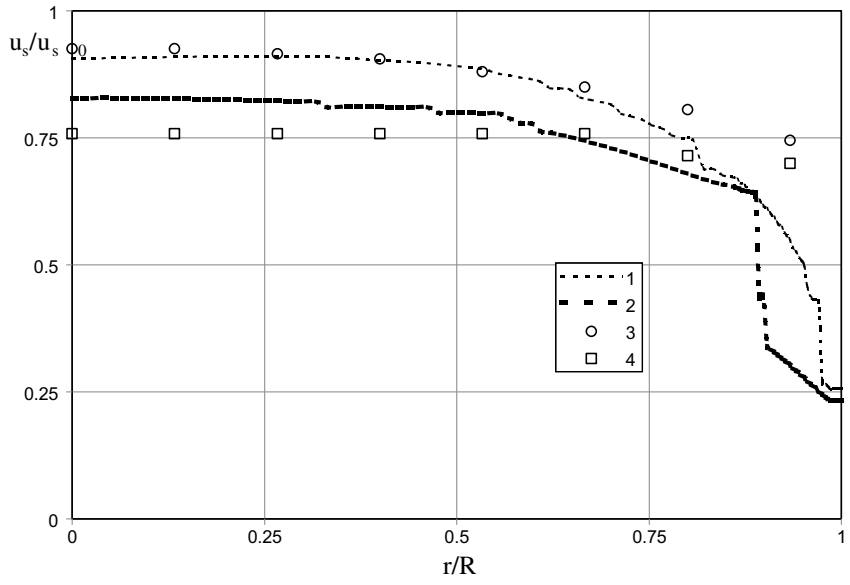

Fig. 4. Profiles of the longitudinal velocity components of particles without the collisions effects: $\delta = 243$ μm (curve 1), $\delta = 501$ μm (curve 2). The experimental data are from Tsuji et al. (1984).

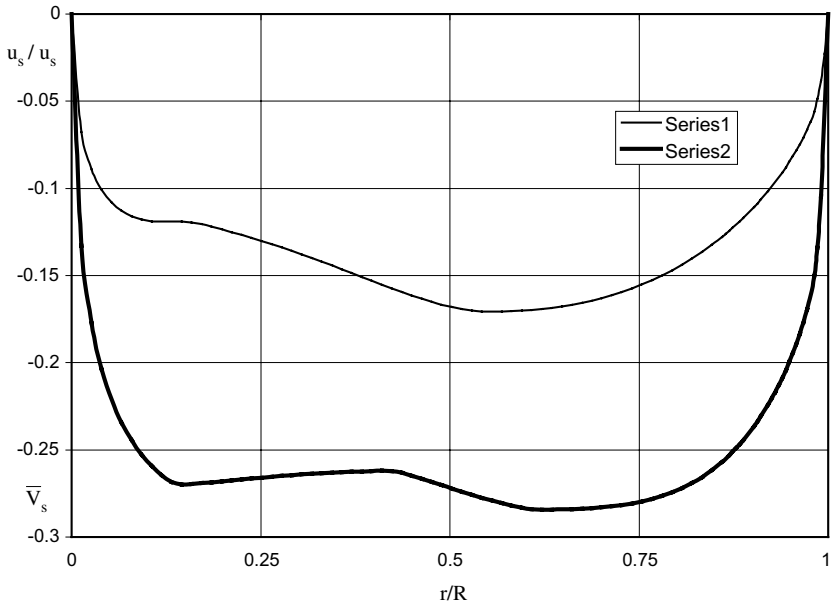

Fig. 5. The profiles of the transverse velocity of particles $\delta = 243$ μm (curve 1), $\delta = 501$ μm (curve 2) along the pipe radius in steady-state flow.

diagram of the mass concentration of particles in a cross-section, which is depicted in Fig. 6. It is observed that the migration of the particles to the center of the pipe is more pronounced in the case of bigger particles.

The distribution of the normalized turbulent intensity is shown in Fig. 7, together with the data by Tsuji et al. (1984). For comparison purposes the intensity for the single-phase flow is also presented. It appears that the model describes adequately, among other things, the turbulence modulation for both the reduction, which is caused predominantly by the finer particles, and for the enhancement of turbulence, which is caused predominantly by the coarser particles.

Fig. 8 shows the calculated values for the distributions of the turbulent viscosity of the fluid and the pseudo-viscosity coefficient for the particles. The data by Tsuji et al. (1984), who measured only the stream-wise velocity fluctuations, are also shown for a qualitative comparison. Although the results are for the quantity $(2k/3)^{1/2}$ and the data represent the quantity $(u'^2)^{1/2}$ the general trends in the graphs are the same. Fig. 9 depicts the turbulent diffusion coefficients of the particles and the pseudo-diffusion coefficient of the dispersed phase. Although there are no experimental data to compare these quantities, the numerical values shown in the figure, the trends and other salient features of the computations appear to be reasonable and the distributions appear as expected in vertical pipe flows.

Finally, Fig. 10 shows an example for the application of the model to the case of a polydisperse mixture of particles. The concentration of particles is shown in the case of two systems, both flowing with the same particle loading. The first system is the monodisperse system of the 501 μm particles, which is also shown in Fig. 7, and the second system is a polydisperse system, composed of equal mass fractions (33.3%) of particles with diameters $\delta = 50$, 100, and 500 μm. It is observed

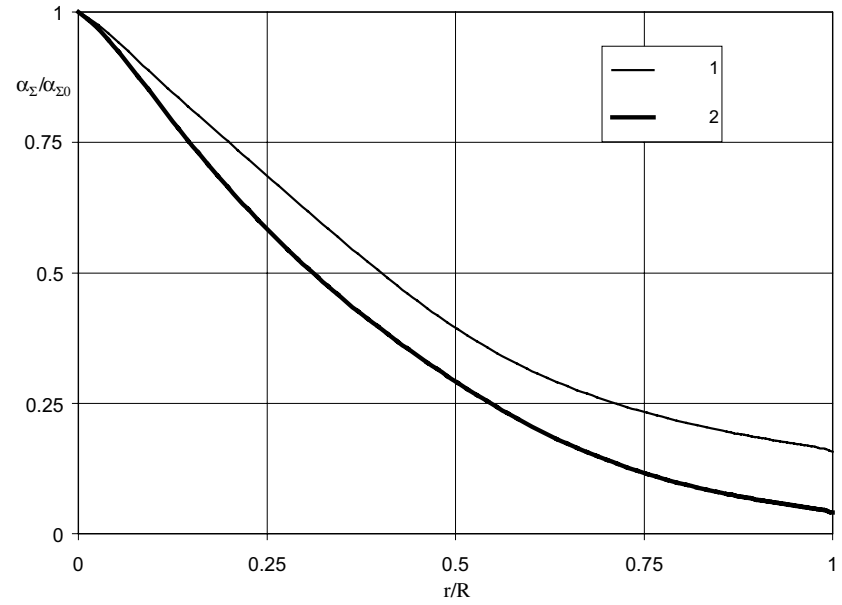

Fig. 6. Profiles for the volumetric concentration of particles with $\delta = 243$ μm (curve 1), and $\delta = 501$ μm (curve 2) along the pipe radius in steady-state flow.

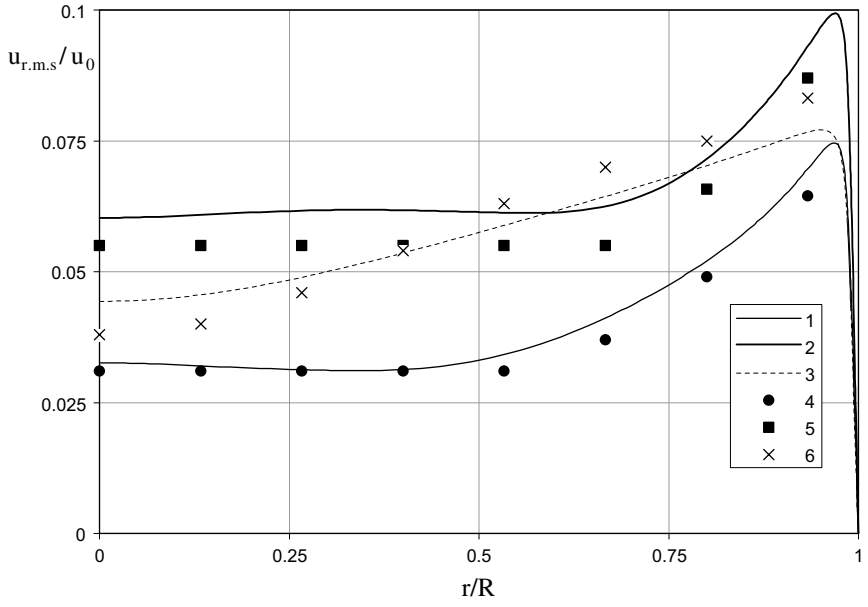

Fig. 7. Turbulence intensity of the carrier fluid with particles: $\delta = 243$ μm (curve 1), $\delta = 501$ μm (curve 2), and without particles (curve 3). The experimental data are from Tsuji et al. (1984).

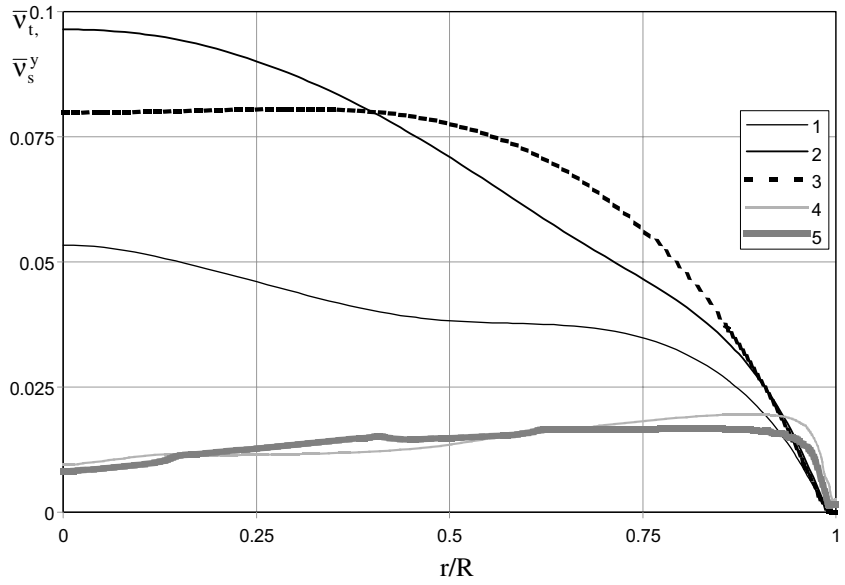

Fig. 8. Coefficient of turbulent viscosity of the carrier fluid with particles: $\delta = 243$ μm (curve 1), $\delta = 501$ μm (curve 2) and without particles (curve 3); and for the pseudo-viscosity of the dispersed phase: $\delta = 243$ μm (curve 4) and $\delta = 501$ μm (curve 5).

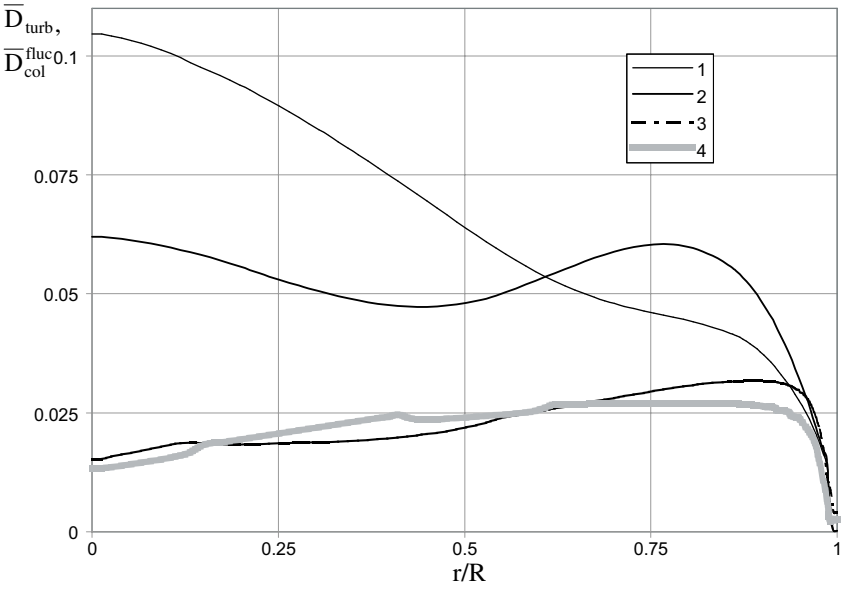

Fig. 9. Turbulent diffusion coefficient of particles: $\delta = 243$ μm (curve 1), $\delta = 501$ μm (curve 2); and pseudo-diffusion coefficients of the dispersed phase: $\delta = 243$ μm (curve 3), $\delta = 501$ μm (curve 4).

that the presence of smaller particles tends to make the flowing properties of the mixture more homogeneous. The apparent lower concentration of the polydisperse system is due to the fact that

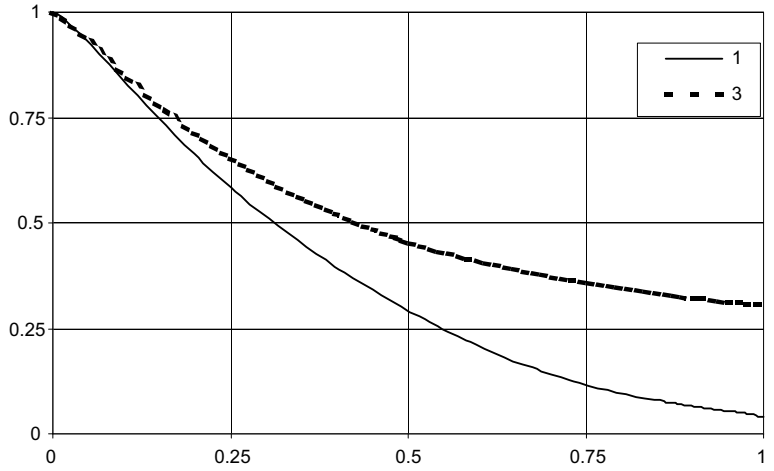

Fig. 10. Profiles of the particle volumetric concentration: monodisperse mixture—$\delta = 501$ μm, $\beta = 100\%$ (curve 1); polydisperse mixture $\delta = 50$ μm, $\beta = 33.3\%$, $\delta = 100$ μm, $\beta = 33.3\%$, and $\delta = 500$ μm, $\beta = 33.3\%$ (curve 3).

the smaller particles move with higher velocity, which is closer to the fluid velocity and, hence, for the same mass flow rate, their local volumetric concentration must be lower.

Regarding the sensitivity of the model to the parameters used, we have performed computations at very high loadings, up to 100, which correspond to average concentrations in the range from 10% to 15%. The results show that the model is robust with respect to the empirical parameters used, up to these high values of the concentration.

6. Conclusions

An algebraic model for the closure of the transport equations of the dispersed phase in a gas–solid mixture is obtained in the general framework of a two-fluid approach. The model takes into account inter-particle collisions as well as particle collisions with the wall. The model applies two mechanisms for the inter-particle collisions, namely sliding friction collision and non-sliding friction collision. This application renders the model more flexible to be used with different flow conditions and applications with different particle fractions. The stress tensor components and the pseudo-viscosity coefficients are analytically obtained and the resulting set of equations is used for the closure of the conservation equations for the mass, the linear momentum and the angular momentum of the solid phase. The numerical computations for a two-phase turbulent upward pipe flow agree well with the experimental data by Tsuji et al. (1984) and reproduce all the salient features of the experimental trends. The model may be further expanded to include computations for the calculation of the particle motion of polydisperse gas–solid flows.

Acknowledgements

This research was made possible by two visits of the first author to Tulane University, which were partly supported by two grants from the ONR and USGS to the Tulane-

Xavier Center for Bioenvironmental research and the Southcentral Regional Center of the National Institute for Global Environmental Change. The research was also supported by the Estonian Ministry of Education, grant number 0070055s98. The authors are grateful for this support.

References

Babukha, G., Shraiber, A., 1972. An interaction of particles of polydisperse composition of materials in a two-phase flow. Naukova Dumka, Kiev.

Crowe, C.T., Gillandt, I., 1998. Turbulence modulation of fluid-particle flows—a basic approach. Third Int. Conf. on Multiphase Flows, Lyon.

Crowe, C.T., Troutt, T.R., Chung, J.N., 1996. Numerical models for two-phase turbulent flows. Ann. Rev. Fluid Mech. 28, 11–43.

Crowe, C., Sommerfeld, M., Tsuji, M., 1998. Multiphase Flows with Droplets and Particles. CRC Press, Boca Raton, FL.

Feng, Z.-G., Michaelides, E.E., 2002. Hydrodynamic force on spheres in cylindrical and prismatic enclosures. Int. J. Multiphase Flow 28, 479–496.

Frishman, F., Hussainov, M., Kartushinsky, A., Mulgi, A., 1997. Numerical simulation of a two-phase turbulent pipe-jet flow loaded with polyfractional solid admixture. Int. J. Multiphase Flow 23, 765–796.

Hussainov, M., Kartushinsky, A., Mulgi, A., Rudi, Ü., Tisler, S., 1995. Experimental and theoretical study of the distribution of mass concentration of solid particles in the two-phase laminar boundary layer on a plate. Int. J. Multiphase Flow 21, 1141–1161.

Hussainov, M., Kartushinsky, A., Mulgi, A., Rudi, Ü., Tisler, 1996. Gas–solid flow with the slip velocity of particles in a horizontal channel. J. Aerosol Sci. 27, 41–59.

Jenkins, J.T., Savage, S.B., 1983. A theory for rapid granular flow of identical, smooth, nearly elastic, spherical particles. J. Fluid Mech. 130, 187–202.

Louge, M.Y., Mastorakos, E., Jenkins, J.T., 1991. The role of particle collisions in pneumatic transport. J. Fluid Mech. 231, 345–359.

Marble, F.E., 1964. Mechanism of particle collision in one-dimensional dynamics of gas–particle admixture. Phys. Fluids 7, 1270–1282.

Matsumoto, S., Saito, S.J., 1970. Monte Carlo simulation of horizontal pneumatic conveying based on the rough wall model. Chem. Eng. Jpn. 3 (2), 223–230.

Mei, R., 1992. An approximate expression for the shear lift force on a spherical particle at finite Reynolds number. Int. J. Multiphase Flow 18, 145–147.

Michaelides, E.E., 2003. Hydrodynamic force and heat/mass transfer from particles, bubbles and drops—the Freeman Scholar Lecture. J. Fluids Eng. 125, 209–238.

Rubinow, S.I., Keller, J.B., 1961. The transverse force on a spinning sphere moving in a viscous fluid. J. Fluid Mech. 11, 447–459.

Saffman, P.G., 1965. The lift on a small sphere in a slow shear flow. J. Fluid Mech. 22, 385–398.

Shiller, L., Naumann, A., 1933. Über die grundlegenden Berechungen bei der Schwerkraftaufbereitung. Ver. Deut. Ing. 77, 318–320.

Shraiber, A.A., Yatsenko, V.P., Gavin, L.B., Naumov, V.A., 1990. Turbulent Flows in Gas Suspensions. Hemisphere, New York.

Sommerfeld, M., 2001. Validation of a stochastic Lagrangian modelling approach for inter-particle collisions in homogeneous isotropic turbulence. Int. J. Multiphase Flow 27, 1829–1858.

Thorncroft, G.E., Klausner, J.F., Mei, R., 2001. Bubble forces and detachment models. Multiphase Sci. Tech. 13 (3–4), 35–76.

Tsuji, Y., Morikawa, Y., Shiomi, H., 1984. LDV measurements of an air–solid two-phase flow in a vertical pipe. J. Fluid Mech. 139, 417–434.

Williams, J.J.E., Crane, R.I., 1983. Particle collision rate in turbulent flow. Int. J. Multiphase Flow 9, 421–435.
Yamomoto, Y., Potthoff, M., Tanaka, T., Kajishima, T., Tsuji, Y., 2001. Large-eddy simulation of turbulent gas–particle flow in a vertical channel: effect of considering inter-particle collisions. J. Fluid Mech. 442, 303–334.
Yuan, Michaelides, E.E., 1992. Turbulence modulation in particulate flows—a theoretical approach. Int. J. Multiphase Flow 18, 779–791.